

The biaxial creep measurement of thin walled tubes

B. D. CLAY

Central Electricity Generating Board, Berkeley Nuclear Laboratories, Berkeley, Gloucestershire, UK

Special features of the design and operation of an apparatus to monitor the biaxial strain of thin walled tubes continuously at temperatures up to 1000°C are described. Secondary creep measurements obtained on circumferentially ribbed tubes of 20/25/Nb stainless steel, used as reactor fuel cladding, are shown to be consistent with recent uniaxial data for the same material, when the biaxial results are expressed in terms of a generalized hoop stress.

1. Introduction

Most of the creep data available for the assessment of the performance of thin-walled tube components originate from conventional tensile tests. However, in service, these components are generally subject to biaxial stresses due to internal and external gas pressures and it is often the case that, in predictions of endurance, the uniaxial data are not correctly applied to the biaxial situation. Further, where biaxial creep data are available, it is usually derived indirectly from stress-rupture tests in which the strain is only measured at failure.

This paper describes an apparatus designed to monitor continuously the diametral straining of tube specimens with internal and external pressurization. The specific purpose of the rig was the measurement of primary and secondary creep in the circumferentially ribbed tubes of 20/25/Nb stainless steel which are the fuel cladding for the Advanced Gas Cooled Reactors (AGR). The secondary creep data obtained on these tube specimens are compared with available uniaxial data for the same material and the relationship between the hoop and uniaxial stress-rates is confirmed. There is also an examination of the effect of circumferential ribs on the calculation of hoop stresses, using a direct comparison between ribbed and smooth tubes of the same material.

2. General description

The basic features of the apparatus are shown in Fig. 1. The tube specimen is located centrally in a

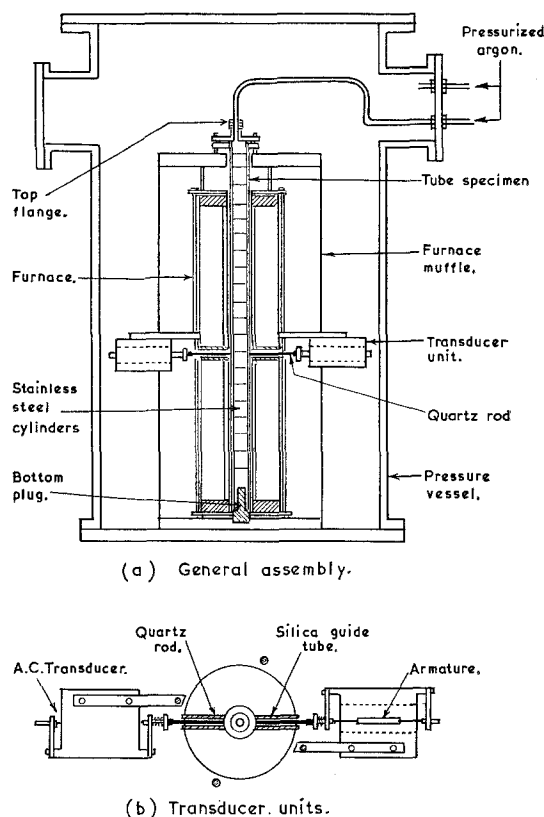


Figure 1 Biaxial strain monitoring rig.

cylindrical furnace which has been modified to allow two quartz rods to be inserted into the hot zone. These rods, 3 mm in diameter, slide in silica guide tubes cemented into the furnace. The

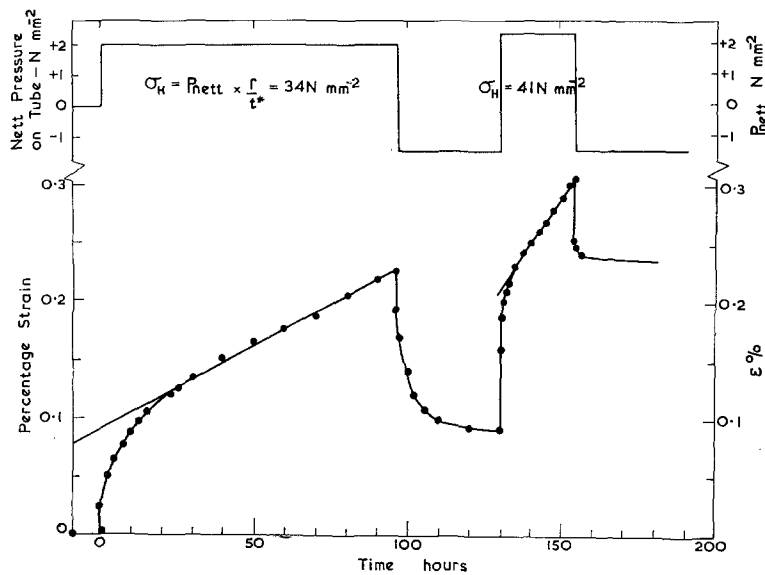


Figure 2 Typical strain-time plots for the biaxial creep tests.

tapered end of each rod is in contact with the specimen and the other with the spring-loaded armature of an a.c. displacement transducer which is clamped in a holder attached to the furnace frame; the transducers can measure to 3×10^{-5} mm over a range of ± 2.5 mm. The insertion of the transducer rods into the hot zones disturbs the regular spacing of the furnace windings. This, together with local convection currents along the guide tubes, can cause a non-uniform distribution of temperature in the region of strain monitoring. This is overcome by winding the furnace in four zones and adjusting the current in each zone by ballast resistors. The maximum current, regulated by a conventional three-term temperature controller, allows temperatures of up to 1000°C to be achieved.

The entire assembly is contained in a 400 mm diameter pressure vessel (Fig. 1) with three side ports for electrical breakthroughs and pressure piping. A control circuit allows the vessel to be pressurized with high purity argon to 4 N mm^{-2} (600 psi) and the specimen tube to 15 N mm^{-2} (2000 psi). In order to minimize the convection currents due to the circulating argon, all the free volume of the vessel is filled either with segmented blocks of refractory cement or with insulating ceramic fibre packing.

3. Specimen preparation

The rig is designed to test smooth or ribbed tubes of about 500 mm length with diameters up to 20

mm. A stainless steel plug is brazed into one end of the tube and a steel flange onto the other (Fig. 1). The tube is filled with close-fitting stainless steel cylinders to prevent collapse of the tube under the external pressure. Ten sheathed thermocouples are spot welded to the assembled specimen to monitor and control the longitudinal and circumferential temperature distributions in the vicinity of the transducer probes.

4. Biaxial creep tests

The pattern of tests is illustrated in Fig. 2. The vessel is pressurized to about 1.5 N mm^{-2} (220 psi) and the pressure equalized in the tube while the optimum temperature distribution is achieved: typically this is $\pm \frac{1}{8}\%$ of the test temperature for 15 mm above and below the transducer rod positions with a similar circumferential distribution. The pressure in the tube is then increased to the required level in less than 2 sec and the test continued at constant pressure until steady-state creep, obtained from monitoring the mean diametral strain, is well established. At the end of the test the gas in the tube is released instantaneously and the cladding allowed to contract under the external pressure. When the contraction slows to a very low rate the tube is repressurized for the next test (Fig. 2). This procedure can be repeated for a series of hoop stresses. When the net strain is 2 to 3% the creep down onto the stainless steel cylinders can

be accelerated by increasing the temperature or external pressure.

At plastic strains in excess of 1% a correction must be applied to the calculated hoop stress to allow for wall thinning: at a hoop strain, ϵ , the original can radius is increased by $(1 + \epsilon)$ and the wall thickness, t , reduced by an equal amount, so that the hoop stress for an internal pressure, p , is given by:

$$\sigma_H = p \cdot \frac{r}{t} (1 + \epsilon)^2. \quad (1)$$

5. Measurements on ribbed tubes

For circumferentially ribbed tubes such as those used for CAGR cladding, it is usually assumed that the rib area is smeared uniformly over the tube surface so that the wall thickness is increased to t^* where

$$t^* = t + \frac{a \cdot b}{p} \quad (2)$$

a , b and p being the rib width, height and spacing respectively. The validity of this "rib-factor" correction has been tested using the biaxial creep rig. The secondary creep rate was measured at 785°C for both ribbed and smooth tubes of the

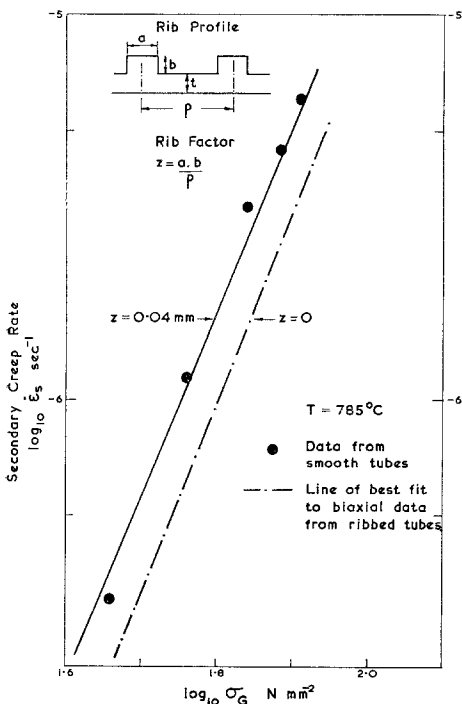


Figure 3 The "Rib factor" correction for circumferentially ribbed tubes.

same material – 20/25/Nb stainless steel. Fig. 3 shows the lines of best fit to the ribbed tube data where the hoop stresses have been calculated from Equation 1 assuming, in one case, no additional rib thickness factor and in the other, a rib factor of 0.04 mm, calculated from the rib dimensions, increasing the effective thickness by 10%. It is seen that the data for the smooth tubes are in good agreement with the corrected line of best fit.

6. Comparison with uniaxial data

The apparatus has been successfully used in an extensive programme of tests on 20/25/Nb

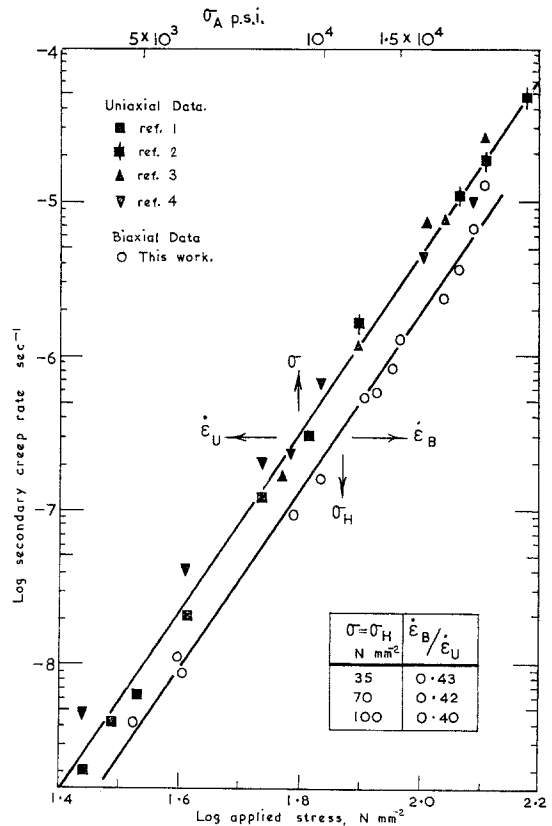


Figure 4 Comparison of biaxial creep data with uniaxial measurements for 20/25/Nb stainless steel (0.05% C) at 750°C.

stainless steel fuel cladding. Fig. 4 compares the secondary creep data obtained at 750°C with recent uniaxial creep measurements [1-4] on similar material at the same temperature. It can be seen that the hoop strain-rate ($\dot{\epsilon}_B$), plotted as a function of hoop stress, is consistently slower than the uniaxial strain-rate ($\dot{\epsilon}_U$) at the same value

of applied stress. The difference can be resolved if it is considered that plastic deformation is due to a generalized stress (σ_G) defined by the von Mises function:

$$\sigma_G = \frac{1}{\sqrt{2}} [(\sigma_1 - \sigma_2)^2 + (\sigma_2 - \sigma_3)^2 + (\sigma_3 - \sigma_1)^2]^{\frac{1}{2}}. \quad (3)$$

For a thin-walled tube, the hoop stress $\sigma_H = \sigma_1 = 2\sigma_2$ and $\sigma_3 \sim 0$ [5], so that

$$\sigma_G = \frac{\sqrt{3}}{2} \sigma_H. \quad (4)$$

Assuming that, for the uniaxial case, the steady-state creep rate varies with stress as

$$\dot{\epsilon}_u = A\sigma^n$$

then for the biaxial case, the hoop strain-rate, which is proportional to the deviatoric stress in that direction [5], is given by

$$\begin{aligned} \dot{\epsilon}_B &= A\sigma_G^{n-1}[\sigma_1 - \frac{1}{2}(\sigma_2 + \sigma_3)] \\ &= \frac{\sqrt{3}}{2} \cdot A\sigma_H^n. \end{aligned} \quad (6)$$

Hence for the same value of applied stress (i.e. $\sigma = \sigma_H$)

$$\dot{\epsilon}_B = \left(\frac{\sqrt{3}}{2}\right)^{n+1} \cdot \dot{\epsilon}_u. \quad (7)$$

For the data at 750°C, the stress exponent $n \simeq 5.5$ so that Equation 5 gives $\dot{\epsilon}_B/\dot{\epsilon}_u \sim 0.4$, which is in fair agreement with the average measured values given in Fig. 4. Thus, when applying uniaxial creep data to the assessment of, for example, fuel cladding endurance, the relevant creep rate is that corresponding to the

generalized hoop stress given by Equation 4. Since creep properties are extremely stress-sensitive in the temperature and stress regions characteristic of reactor operation, the omission of this correction to the calculated hoop stress can give estimates of cladding strains and collapse rates which are 3 to 4 times too high.

7. Conclusions

The equipment has performed very satisfactorily throughout the present programme of tests on both ribbed and smooth tube specimens. It is clear that the apparatus is ideally suited for a much wider range of combined creep and fatigue experiments. The continuous monitoring of strain facilitates the measurement of load reversal effects, stress relaxation and stress decrement tests. Furthermore, the apparatus could be easily adapted to investigate more complex stress systems by applying axial loading to the tube.

Acknowledgement

This paper is published by permission of the Central Electricity Generating Board.

References

1. I. R. MCLAUCHLIN, C.E.G.B. Report No. 2152 (1972).
2. *Idem*, C.E.G.B. Report No. 2151 (1971).
3. K. R. WILLIAMS and I. R. MCLAUCHLIN, *J. Mater. Sci.* **5** (1970) 1063.
4. P. A. HITCHCOCK, private communication.
5. A. COTTRELL, "The Mechanical Properties of Matter" (Wiley, New York, 1964) p. 122.

Received 31 January and accepted 19 February 1974.